chemistry proceedings

MDPI

Proceeding Paper

Influence of At-Bridge Nitro Groups on the Photophysics and Chiroptics of helicoBODIPYs: A Step Forward towards the Development of New Chiroptical Sensors †

César Ray [1], Carolina Díaz-Norambuena [2], Christopher Schad [1], Florencio Moreno [1], Antonia R. Agarrabeitia [1,3], María J. Ortiz [1], Teresa Arbeloa [2], Jorge Bañuelos [2], Beatriz L. Maroto [1,*] and Santiago de la Moya [1,*]

1 Departamento de Química Orgánica, Facultad de Ciencias Químicas, Universidad Complutense de Madrid, Ciudad Universitaria s/n, 28040 Madrid, Spain; cesarrayleiva@ucm.es (C.R.); cschad@ucm.es (C.S.); floren@ucm.es (F.M.); agarrabe@ucm.es (A.R.A.); mjortiz@ucm.es (M.J.O.)

2 Departamento de Química Física, Facultad de Ciencia y Tecnología, Universidad del País Vasco-EHU, 48080 Bilbao, Spain; carolina.diaz@ehu.eus (C.D.-N.); teresa.arbeloa@ehu.eus (T.A.); jorge.banuelos@ehu.eus (J.B.)

3 Sección Departamental de Química Orgánica, Facultad de Óptica y Optometría, Universidad Complutense de Madrid, 28037 Madrid, Spain

* Correspondence: belora@ucm.es (B.L.M.); santmoya@ucm.es (S.d.l.M.); Tel.: +34-913944716 (B.L.M.); +34-913945090 (S.d.l.M.)

† Presented at the 25th International Electronic Conference on Synthetic Organic Chemistry, 15–30 November 2021; Available online: https://ecsoc-25.sciforum.net/.

Abstract: A new helicoBODIPY (bisBODIPY with helical chirality) with nitro groups at the chiral bridge has been synthesized as a model to study the influence of the at-bridge substitution on the photophysics and chiroptics of the helicoBODIPY. This preliminary study reveals that at-bridge substitution can be a strategy for the development of chiroptical sensors based on helicoBODIPYs.

Keywords: organic dyes; BODIPY; stereoelectronic effects; photophysics; chiroptics

Citation: Ray, C.; Díaz-Norambuena, C.; Schad, C.; Moreno, F.; Agarrabeitia, A.R.; Ortiz, M.J.; Arbeloa, T.; Bañuelos, J.; Maroto, B.L.; Moya, S.d.l. Influence of At-Bridge Nitro Groups on the Photophysics and Chiroptics of helicoBODIPYs: A Step Forward towards the Development of New Chiroptical Sensors. *Chem. Proc.* **2022**, *8*, 3. https://doi.org/10.3390/ecsoc-25-11701

Academic Editor: Julio A. Seijas

Published: 14 November 2021

1. Introduction

The discovery and exploration of chiroptical phenomena, such as circular dichroism (CD) and circularly polarized luminescence (CPL), has boosted the applicability of chiral systems and their interaction with light in the recent years [1–5], contributing to the development of chiroptics. Optical techniques based on chiroptics have major applications as CP-OLEDs, security inks, systems for the storage and processing of information, and CPL microscopy, among others [6–9].

One of the most interesting fields in which chiroptics has been allowed to advance in science has been chemical analysis, with the so-called chiroptical sensing [10]. This type of sensing, based on CD or CPL specifically, enables analyses with greater sensitivity and resolution than traditional methods, due to the higher definition of circularly polarized light [10]. In addition, its applicability goes beyond the determination of configurations of chiral molecules and also covers important issues such as the determination of conformational arrangements of chiral molecules and detection of chiral or achiral species, as well as the study of the self-assembly of supramolecular structures [11–13].

For the development and implantation of this novel tool it is necessary to have optically active chiral species that can act as sensors [3]. Unfortunately, there is no extensive collection of chiral chromophoric platforms available to date for the synthetic development of chiroptical sensors. The latter, together with the necessary technology and instrumentation, has yet to be developed, which makes the exploitation of chiroptical sensing still a work in progress [14].

In this sense, de la Moya introduced in 2013 a new design based on a bis(BODIPY) with helical chirality provided by a chiral diamine or diol tether (helicoBODIPY, see (*R*,*R*)-**1** as an example in Figure 1) [15]. This design has characteristics with great potential for the development of chiroptical sensors [15,16]. First, its chiroptical behavior, which shows a strongly bisignated signal in the CD spectrum and also a CPL emission in the visible region, with luminescence dissymmetry factor values (g_{lum}, [17]) which fall in the usual range for small organic molecules, and which can be modulated by structural changes in its chiral bridge [16]. This exceptional chiroptical behavior arises from the induction of a pseudohelical conformation in solution, with a preferred configuration induced by the chiral bridge (see Figure 1), which allows an exciton coupling between the two chromophores. Second, its conformational flexibility, which enables the dye to adopt said helical conformation and provides the helicoBODIPY design with great value as a platform for chiroptical sensing. And third, but no less important, its straightforward synthesis from accessible *F*-BODIPYs and enantiopure C_2 symmetric diamines or diols [15,16].

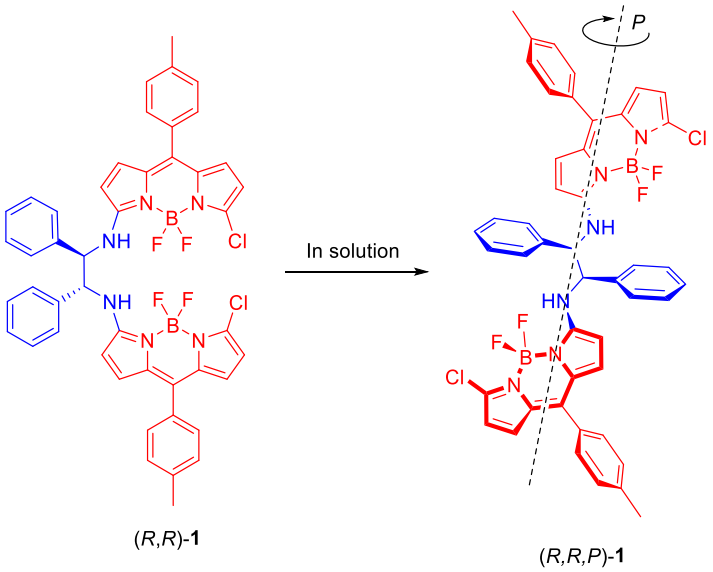

Figure 1. Example of the helicoBODIPY design introduced by de la Moya and its helical conformation with a preferred configuration in solution.

Therefore, we hypothesized that, as the flexible chiral bridge is responsible for providing the helicoBODIPY design with these exceptional chiroptical properties, modifications of the structure or the conformation of the bridge should lead to changes in the chiroptical behavior of the dye. It is precisely based on this foundation that the helicoBODIPY design would carry out its function as a chiroptical sensor: the species to be detected being capable, through specific interactions with the spacer, of inducing changes in the original conformation of the sensor; thus, leading to different chiroptical responses [18–20].

For this purpose, we decided to introduce into the bridge a functional group directed at the construction of chiroptical sensors. This group should be easily transformed into a group suitable for the recognition of analytes, keeping in mind that the introduction of this group should not interfere with the synthetic access to the dye, nor avoid the necessary helical arrangement. The nitro group was considered as a good option, due to its compatibility with the aromatic nucleophilic substitution (S_NAr) reaction involved in the dye synthesis and also due to the ease of derivatization to an amino group by simple hydrogenation (Scheme 1) [21,22]. The amino group has a well-known capability for the recognition of electron deficient analytes [23,24], as well as a rich chemistry that would allow numerous types of reactions directed to increase the applicability of the design.

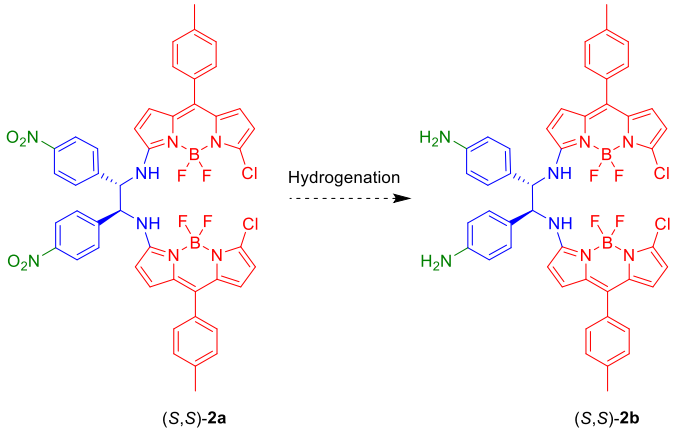

Scheme 1. Rationalization of a new helicoBODIPY-based chiroptical sensor design.

In order to validate the at-bridge-substituted helicoBODIPY design for the future development of chiroptical sensors, it is necessary to study the influence of the nitro groups located at the bridge on the photophysics and chiroptics of the helicoBODIPY. This communication describes the preliminary results of this study, directed at obtaining closer knowledge on the key structural factors that govern the (chir)optical properties of the helicoBODIPY design, which could be of great utility to consolidate this design for the development of chiroptical sensors.

2. Results and Discussion

The synthesis of helicoBODIPY (*S*,*S*)-**2a** was carried out following the methodology developed by us for the synthesis of **1**, based on a double S_NAr of chlorine in 3,5-dichloro-4,4-difluoro-8-(4-methylphenyl)BODIPY (**3**) [25] using (*S*,*S*)-*N*,*N*′-bis(4-nitrophenyl)ethane-1,2-diamine (**4**) as the nucleophile in acetonitrile in the presence of triethylamine. However, the expected product (*S*,*S*)-**2a** was not obtained, not even at a refluxing temperature, probably due to the lower nucleophilicity of the diamine when compared to the unsubstituted one in the synthesis of **1** (owing to the electron-withdrawing nitro groups). Fortunately, the application of more vigorous reaction conditions (refluxing dioxane) led to bis(BODIPY) (*S*,*S*)-**2a** in a satisfactory 44% yield (Scheme 2).

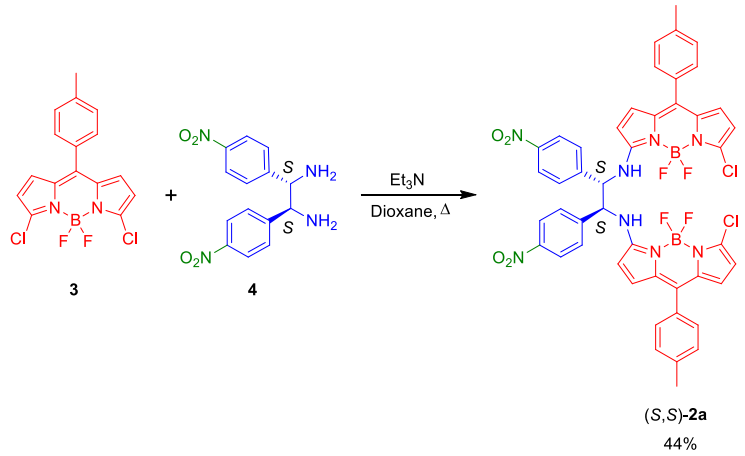

Scheme 2. Synthesis of (*S*,*S*)-**2a**.

The study of the photophysical properties of new dye **2a** was performed in comparison with its unsubstituted analogue **1** [15], in order to evaluate whether the introduction of substituents into the structure of the bridge could alter the photophysics of the helicoBODIPY. Fortunately, as can be observed in Table 1, the photophysical signatures of both dyes did not differ much. The presence of the nitro groups in the diamine bridge of **2a** seemed to

induce a slight bathochromic shift of the spectral bands in relation to **1**, which could be related to changes in the probability of the vibrational transitions.

Table 1. Comparative spectroscopic data for **1** and **2a** in different solvents (*ca.* 10^{-6} M).

Dye	Solvent	λ_{ab} [a] (nm)	ε_{max} [b] (10^4 $M^{-1}cm^{-1}$)	λ_{fl} [c] (nm)	ϕ [d]	τ [e] (ns)
1 [f]	*c*-hexane	529.0	12.4	544.0	0.17	1.15 (97%) 4.70 (3%)
	chloroform	525.5	8.3	544.5	0.14	0.23 (32%) 1.15 (68%)
	acetone	508.5 469.5	5.5 5.8	537.5	0.005	–
	methanol	511.0 469.5	5.4 5.5	535.5	0.001	–
2a	*c*-hexane	534.0 495.0	8.0 4.2	546.5	0.23	1.50 (96%) 5.03 (4%)
	chloroform	532.5 492.5	8.4 5.1	548.0	0.07	0.18 (42%) 0.75 (58%)
	acetone	512.0 473.5	5.0 5.4	537.5	0.003	–
	methanol	514.5 474.0	4.9 5.2	539.5	0.003	–

[a] Maximum absorption wavelength. [b] Maximum molar absorptivity. [c] Maximum fluorescence wavelength. [d] Fluorescence quantum yield. [e] Fluorescence lifetime. [f] Data from ref. [26].

Regarding the fluorescence response, a similar behavior was observed for **2a** and **1**. The fluorescence quantum yield decreased when the polarity of the medium increased for both dyes. This is evidence of an intramolecular charge transfer (ICT) in the excited state, which has higher probability in polar media [15]. As the nitro substituents are not π-conjugated with the nitrogens of the diamine, these groups do not have significant influence on the ongoing ICT.

The CD spectrum of the new dye (*S*,*S*)-**2a** was similar to that of its analogue (*S*,*S*)-**1** [15] (Figure 2). It provided a comparable bisignalized signal, with a positive Cotton effect, demonstrating the formation of a helical conformation in solution with a preferred *M* configuration. Therefore, the introduction of the *p*-nitro groups at the phenyl units of the bridge does not affect the induced axial stereochemistry of the dye in solution. However, it does induce a change in the degree of the differential absorption of circular polarized light, being the maximum absorption dissymmetry ratio, g_{abs} [27], for (*S*,*S*)-**2a** ($+3.8 \times 10^{-3}$, in chloroform) twice the value of g_{abs} for (*S*,*S*)-**1** ($+1.6 \times 10^{-3}$, in chloroform). This result shows that changes in the structure of the bridge can induce changes in the degree of the CD absorption, or in other words, changes in the chiroptical response of the dye, which is a behavior that is sought when developing chiroptical sensors.

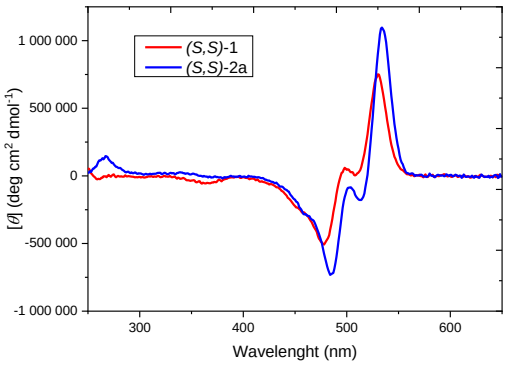

Figure 2. Circular dichroism spectra of (*S*,*S*)-**1** (red) and (*S*,*S*)-**2a** (blue) in chloroform (4×10^{-6} M).

3. Conclusions

A new helicoBODIPY (*S*,*S*)-**2a** has been designed and obtained. This helicoBODIPY is based on the previously described (*S*,*S*)-**1** [15], but includes a chiral diamino bridge with nitro groups for its future derivatization to amino groups, directed at the development of sensors. The new dye could be straightforwardly obtained following the previously described procedure for the synthesis of helicoBODIPYs and it kept the photophysical properties of parent **1**. It also provided a similar chiroptical response in CD, a consequence of the formation of a helical conformation in solution, with the same preferred configuration as parent **1** but with changes in the polarization degree, as detected by the measured g_{abs} value. The observed change in the g_{abs} value, caused by a change in the structure of the bridge, could be used for the development of chiroptical sensors based on CD.

4. Materials and Methods

4.1. Synthetic Procedures

General: Common solvents were dried and distilled by standard procedures. All starting materials and reagents were obtained commercially and used without further purifications. Elution flash chromatography was conducted on silica gel (230 to 400 mesh ASTM). Thin layer chromatography (TLC) was performed on silica gel plates (silica gel 60 F254, supported on aluminum). The NMR spectra were recorded at 20 °C. The residual solvent peaks were used in ^{1}H NMR ($CDCl_3$: δ 7.26 ppm) and ^{13}C NMR ($CDCl_3$: δ 77.16 ppm)as internal standards, and external standards were used in ^{11}B NMR (15% $BF_3{\cdot}OEt_2$ in $CDCl_3$: δ 0.00 pm) and in ^{19}F NMR (0.05% trifluorotoluene in $CDCl_3$: δ − 62.72 ppm). The NMR signals are given in ppm. DEPT-135 NMR experiments were used for the assignation of the type of carbon nucleus (C, CH, CH_2, or CH_3). The FTIR spectra were recorded from neat samples using the ATR technique and IR bands are given in cm^{-1}. The measurement of the optical rotations was performed in quartz cells of 1 dm length and 1mL capacity. For the specific rotation, $[\alpha]_D^t$ (where t is the temperature in °C and D refers to the sodium spectral line used, 589 nm), the concentration *c* (in g/100 mL) and the solvent are given. CD spectra were recorded on a Jasco (model J-715) spectropolarimeter using standard quartz cells of 1 cm optical-path length in chloroform solution, unless otherwise indicated, at a dye concentration of ca. 4×10^{-6} M.

Synthesis of (*S*,*S*)-**2a**: A mixture of 3,5-dichloro-4,4-difluoro-8-(4-methylphenyl)BODIPY (**3** [25]; 50 mg, 0.143 mmol), (*S*,*S*)-*N*,*N*′-bis(4-nitrophenyl)ethane-1,2-diamine (**4**; 25.5 mg, 0.068 mmol), and triethylamine (58 mg, 0.572 mmol) in dry dioxane (3 mL) was refluxed under argon for 3.5 h. After cooling the reaction mixture to room temperature, CH_2Cl_2 (15 mL) and water (15 mL) were added, the organic layer was separated, and the aqueous layer was extracted with CH_2Cl_2 (2 × 10 mL). The combined organic phases were then washed with water (1 × 15 mL) and brine (1 × 15 mL) and dried over anhydrous Na_2SO_4. After filtration and solvent evaporation under reduced pressure, the obtained residue was purified by flash chromatography (CH_2Cl_2). (*S*,*S*)-**2a**: 29 mg (44%). Brown solid. R_f = 0.10 (hexane/CH_2Cl_2 1:1). $[\alpha]_D^{20}$ +6093.6 (*c* 0.104, $CHCl_3$). ^{1}H NMR ($CDCl_3$, 300 MHz) δ 8.12 (d, *J* = 8.4 Hz, 4H), 7.66 (br s, 2H), 7.28 (m, 4H), 7.12 (m, 8H), 6.63 (d, *J* = 4.9 Hz, 2H), 6.44 (d, *J* = 4.0 Hz, 2H), 6.26 (d, *J* = 4.0 Hz, 2H), 5.65 (d, *J* = 4.9 Hz, 2H), 5.20 (m, 2H), 2.41 (s, 6H) ppm. ^{13}C NMR ($CDCl_3$, 75 MHz) δ 160.2 (C), 148.3 (C), 144.4 (C), 139.9 (C), 135.6 (CH), 134.9 (C), 132.7 (C), 132.1 (C), 130.5 (C), 130.2 (br s, CH), 129.2 (CH), 128.8 (CH), 124.4 (CH), 122.7 (CH), 113.9 (CH), 110.1 (CH), 62.5 (CH), 21.5 (CH_3) ppm. ^{11}B NMR ($CDCl_3$, 160 MHz) δ 0.83 (s) ppm. ^{19}F NMR ($CDCl_3$, 471 MHz) δ −146.2 (br s), −148.1 (m) ppm. FTIR ν 1590, 1524, 1488, 1348, 1096 cm^{-1}.

4.2. Spectroscopic Measurements and Quantum Mechanic Calculations

The photophysical properties were registered using quartz cuvettes with optical pathways of 1 cm in diluted solutions (around 2×10^{-6} M), prepared by diluting the concentrated stock solution in acetone. Ultraviolet-visible (UV-vis) absorption and fluorescence spectra were recorded on a Varian model CARY 4E spectrophotometer and an

Edinburgh Instruments spectrofluorometer (model FLSP920), respectively. Fluorescence quantum yields (ϕ) were obtained using PM546 (Exciton, $\phi^r = 0.85$), and obtained in ethanol as the reference. Radiative decay curves were registered with the time-correlated single-photon counting technique, as implemented in the aforementioned spectrofluorometer. Fluorescence emission was monitored at the maximum emission wavelength, by means of a microchannel plate detector (Hamamatsu C4878) of picosecond time-resolution (20 ps) after excitation with a wavelength-tunable Fianium pulsed laser (time resolution of around 150 ps). The fluorescence lifetime (τ) was obtained after the deconvolution of the instrumental response signal from the recorded decay curves by means of an iterative method. The goodness of the exponential fit was controlled by statistical parameters (chi-square) and the analysis of the residuals.

Author Contributions: Conceptualization, S.d.l.M. and B.L.M.; Synthesis, C.R. and C.D.-N.; NMR and IR studies, C.S. and M.J.O.; chiroptics: F.M. and A.R.A.; photophysics: J.B., T.A. and C.D.-N.; writing—original draft preparation, C.R., C.S. and C.D.-N.; writing—review and editing, S.d.l.M., B.L.M. and J.B.; funding acquisition, S.d.l.M., M.J.O. and J.B. All authors have read and agreed to the published version of the manuscript.

Funding: Financial support from the Ministerio de Ciencia e Innovación of Spain (MAT2017-83856-C3-2-P and -3-P and PID2020-114755GB-C32 and -C33) and Gobierno Vasco (IT912-16) is gratefully acknowledged. C.R. and C.S. each thank Comunidad de Madrid-UCM for research contracts. C.D.-N. thanks the Ministerio de Ciencia e Innovación of Spain for a FPI predoctoral fellowship.

Conflicts of Interest: The authors declare no conflict of interest. The funders had no role in the design of the study; in the collection, analyses, or interpretation of data; in the writing of the manuscript, or in the decision to publish the results.

References and Notes

1. Martin, S.R.; Schilstra, M.J. Circular Dichroism and Its Application to the Study of Biomolecules. In *Methods in Cell Biology*; Academic Press: Cambridge, MA, USA, 2008; Volume 84, pp. 263–293.
2. Maupin, C.L.; Riehl, J.P. Circularly Polarized Luminescence and Fluorescence Detected Circular Dichroism. In *Encyclopedia of Spectroscopy and Spectrometry*; Elsevier: Amsterdam, The Netherlands, 2017; pp. 305–311.
3. Mori, T. (Ed.) *Circularly Polarized Luminescence of Isolated Small Organic Molecules*; Springer: Singapore, 2020.
4. Sang, Y.; Han, J.; Zhao, T.; Duan, P.; Liu, M. Circularly Polarized Luminescence in Nanoassemblies: Generation, Amplification, and Application. *Adv. Mater.* **2020**, *32*, 1900110. [CrossRef] [PubMed]
5. Zinna, F.; Giovanella, U.; Bari, L.D. Highly Circularly Polarized Electroluminescence from a Chiral Europium Complex. *Adv. Mater.* **2015**, *27*, 1791–1795. [CrossRef] [PubMed]
6. MacKenzie, L.E.; Pal, R. Circularly Polarized Lanthanide Luminescence for Advanced Security Inks. *Nat. Rev. Chem.* **2021**, *5*, 109–124. [CrossRef]
7. Amako, T.; Nakabayashi, K.; Suzuki, N.; Guo, S.; Rahim, N.A.A.; Harada, T.; Fujiki, M.; Imai, Y. Pyrene Magic: Chiroptical Enciphering and Deciphering 1,3-Dioxolane Bearing Two Wirepullings to Drive Two Remote Pyrenes. *Chem. Commun.* **2015**, *51*, 8237–8240. [CrossRef] [PubMed]
8. Andres, J.; Hersch, R.D.; Moser, J.-E.; Chauvin, A.-S. A New Anti-Counterfeiting Feature Relying on Invisible Luminescent Full Color Images Printed with Lanthanide-Based Inks. *Adv. Funct. Mater.* **2014**, *24*, 5029–5036. [CrossRef]
9. Koike, H.; Nozaki, K.; Iwamura, M. Microscopic Imaging of Chiral Amino Acids in Agar Gel through Circularly Polarized Luminescence of Eu^{III} Complex. *Chem. Asian J.* **2020**, *15*, 85–90. [CrossRef]
10. Ozcelik, A.; Pereira-Cameselle, R.; Poklar Ulrih, N.; Petrovic, A.G.; Alonso-Gómez, J.L. Chiroptical Sensing: A Conceptual Introduction. *Sensors* **2020**, *20*, 974. [CrossRef] [PubMed]
11. Hache, F.; Changenet, P. Multiscale Conformational Dynamics Probed by Time-resolved Circular Dichroism from Seconds to Picoseconds. *Chirality* **2021**, *33*, 747–757. [CrossRef]
12. Ma, J.-L.; Peng, Q.; Zhao, C.-H. Circularly Polarized Luminescence Switching in Small Organic Molecules. *Chem. Eur. J.* **2019**, *25*, 15441–15454. [CrossRef]
13. Bentley, K.W.; Wolf, C. Comprehensive Chirality Sensing: Development of Stereodynamic Probes with a Dual (Chir)optical Response. *J. Org. Chem.* **2014**, *79*, 6517–6531. [CrossRef]
14. Deng, Y.; Wang, M.; Zhuang, Y.; Liu, S.; Huang, W.; Zhao, Q. Circularly Polarized Luminescence from Organic Micro-/Nano-Structures. *Light Sci. Appl.* **2021**, *10*, 76. [CrossRef] [PubMed]
15. Sánchez-Carnerero, E.M.; Moreno, F.; Maroto, B.L.; Agarrabeitia, A.R.; Bañuelos, J.; Arbeloa, T.; López-Arbeloa, I.; Ortiz, M.J.; de la Moya, S. Unprecedented Induced Axial Chirality in a Molecular BODIPY Dye: Strongly Bisignated Electronic Circular Dichroism in the Visible Region. *Chem. Commun.* **2013**, *49*, 11641–11643. [CrossRef] [PubMed]

16. Ray, C.; Sánchez-Carnerero, E.M.; Moreno, F.; Maroto, B.L.; Agarrabeitia, A.R.; Ortiz, M.J.; López-Arbeloa, Í.; Bañuelos, J.; Cohovi, K.D.; Lunkley, J.L.; et al. Bis(HaloBODIPYs) with Labile Helicity: Valuable Simple Organic Molecules That Enable Circularly Polarized Luminescence. *Chem. Eur. J.* **2016**, *22*, 8805–8808. [CrossRef] [PubMed]
17. The degree of CPL is given by the luminescence dissymmetry ratio, $g_{\mathrm{lum}}(\lambda)=2\Delta I/I = 2(I_{\mathrm{L}} - I_{\mathrm{R}})/(I_{\mathrm{L}} + I_{\mathrm{R}})$, where I_{L} and I_{R} refer, respectively, to the intensity of left and right circularly polarized emissions.
18. Wolf, C.; Bentley, K.W. Chirality Sensing Using Stereodynamic Probes with Distinct Electronic Circular Dichroism Output. *Chem. Soc. Rev.* **2013**, *42*, 5408–5424. [CrossRef]
19. Zardi, P.; Wurst, K.; Licini, G.; Zonta, C. Concentration-Independent Stereodynamic g-Probe for Chiroptical Enantiomeric Excess Determination. *J. Am. Chem. Soc.* **2017**, *139*, 15616–15619. [CrossRef]
20. Zhao, N.; Gao, W.; Zhang, M.; Yang, J.; Zheng, X.; Li, Y.; Cui, R.; Yin, W.; Li, N. Regulation of Circular Dichroism Behavior and Construction of Tunable Solid-State Circularly Polarized Luminescence Based on BINOL Derivatives. *Mater. Chem. Front.* **2019**, *3*, 1613–1618. [CrossRef]
21. Tafesh, A.M.; Weiguny, J. A Review of the Selective Catalytic Reduction of Aromatic Nitro Compounds into Aromatic Amines, Isocyanates, Carbamates, and Ureas Using CO. *Chem. Rev.* **1996**, *96*, 2035–2052. [CrossRef]
22. Orlandi, M.; Brenna, D.; Harms, R.; Jost, S.; Benaglia, M. Recent Developments in the Reduction of Aromatic and Aliphatic Nitro Compounds to Amines. *Org. Process Res. Dev.* **2018**, *22*, 430–445. [CrossRef]
23. Boens, N.; Leen, V.; Dehaen, W. Fluorescent Indicators Based on BODIPY. *Chem. Soc. Rev.* **2012**, *41*, 1130–1172. [CrossRef]
24. Kaur, P.; Singh, K. Recent Advances in the Application of BODIPY in Bioimaging and Chemosensing. *J. Mater. Chem. C* **2019**, *7*, 11361–11405. [CrossRef]
25. Baruah, M.; Qin, W.; Basaric, N.; De Borggraeve, W.M.; Boens, N.L. BODIPY-Based Hydroxyaryl Derivatives as Fluorescent pH Probes. *J. Org. Chem.* **2005**, *70*, 4152–4157. [CrossRef] [PubMed]
26. Ray, C.; Bañuelos, J.; Arbeloa, T.; Maroto, B.L.; Moreno, F.; Agarrabeitia, A.R.; Ortiz, M.J.; Lopez-Arbeloa, I.; de la Moya, S. Push-pull flexibly-bridged bis(haloBODIPYs): Solvent and spacer switchable red emission. *Dalton Trans.* **2016**, *45*, 11839–11848. [CrossRef] [PubMed]
27. The degree of CD is given by the absorbance dissymmetry ratio (Kuhn's dissymmetry ratio), $g_{abs}(\lambda) = 2\Delta\varepsilon/\varepsilon = 2(\varepsilon_{\mathrm{L}} - \varepsilon_{\mathrm{R}})/(\varepsilon_{\mathrm{L}} + \varepsilon_{\mathrm{R}})$, where ε_{L} and ε_{R} refer, respectively, to the molar absorptivity of left and right circularly polarized absorptions.